6-D Localization of a Magnetic Capsule Endoscope Using a Stationary Rotating Magnetic Dipole Field

K. M. Popek[1], J. J. Abbott[2]

[1]*School of Computing,* [2]*Dept. of Mechanical Engineering, University of Utah, USA*
{katie.popek, jake.abbott}@utah.edu

INTRODUCTION

Since the introduction of passive commercial capsule endoscopes, researchers have been pursuing methods to control and localize these devices, many utilizing magnetic fields [1, 2]. An advantage of magnetics is the ability to both actuate and localize using the same technology. Prior work from our group [3] developed a method to *actuate* screw-type magnetic capsule endoscopes in the intestines using a single rotating magnetic dipole located at any position with respect to the capsule. This paper presents a companion *localization* method that uses the same rotating dipole field for full 6-D pose estimation of a capsule endoscope embedded with a small permanet magnet and an array of magnetic-field sensors. Although several magnetic localization algorithms have been previously published, many are not compatible with magnetic actuation [4, 5]. Those that are require the addition of an accelerometer [6, 7], need *a priori* knowledge of the capsule's orientation [7], provide only 3-D information [6], or must manipulate the position of the external magnetic source during localization [8, 9]. Kim et al. presented an iterative method for use with rotating magnetic fields, but the method contains errors [10]. Our proposed algorithm is less sensitive to data synchronization issues and sensor noise than our previous non-iterative method [11] because the data from the magnetic sensors is incorporated independently (rather than first using sensor data to estimate the field at the center of the capsule's magnet), and the full pose is solved simultaneously (instead of position and orientation sequentially).

MATERIALS AND METHODS

Localization is performed relative to the robot's frame, $\boldsymbol{O}_R$, which we place at the location of the rotating dipole (i.e., the center of the actuator magnet). The capsule's coordinate frame origin, $\boldsymbol{O}_C$, which resides at the center of the capsule's magnet, is described by the vector $\boldsymbol{p}_C$ (Fig. 1). The rotation matrix, R, describes the capsule's coordinate frame relative to the robot's. Our goal is to solve for $\boldsymbol{p}_C$ and R.

This method assumes the capsule is free to move, but that the dipole-field rotation is well beyond the "step-out" frequency, where the field is rotating too quickly for the capsule to rotate synchronously, such that we can assume no net motion and decouple the localization and actuation of the capsule. In our setup, the field source is

This material is based upon work supported by the National Science Foundation under Grant No. 0952718.

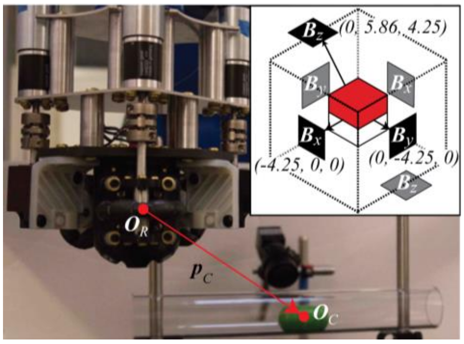

Fig. 1 Experimental setup with a spherical-actuator-magnet manipulator [12], mounted on the end of a 6-DOF robot. A prototype capsule freely rotates and slides in a clear, acrylic, lubricated tube. The inset depicts the capsule's sensor layout [11]. Each sensor is labeled with the field component it measures and its offset, $\boldsymbol{\delta}_i$ in mm, from the internal magnet's center. The grey sensors are not visible from this angle, but are at symmetric offsets.

a spherical permanent magnet, which is accurately modeled by the point-dipole equation [3]:

$$\boldsymbol{B}(\boldsymbol{p}) = \frac{\mu_0}{4\pi\|\boldsymbol{p}\|^3}\left(3\hat{\boldsymbol{p}}\hat{\boldsymbol{p}}^T - I\right)\boldsymbol{M} \qquad (1)$$

where $\boldsymbol{B}(\boldsymbol{p})$ is the field at location $\boldsymbol{p}$, $\hat{\boldsymbol{p}}$ is the unit-normalized $\boldsymbol{p}$ vector, $\boldsymbol{M}$ is the dipole moment of the magnet, I is the identity matrix, and μ_0 is the permeability of free space.

We previously developed an array of six Hall-effect sensors to surround the magnet inside the capsule to estimate the applied field at its location [11] (Fig. 1). The sensors are placed at known offsets, $\boldsymbol{\delta}_i$, as noted in Fig. 1. The position vector, $\boldsymbol{p}_i$, describing sensor i in the robot frame, is $\boldsymbol{p}_i = \boldsymbol{p}_C + R\boldsymbol{\delta}_i$. The scalar magnetic-field projection measured at each sensor is:

$$B_i(\boldsymbol{p}_i) = \boldsymbol{s}_i^T R^T \frac{\mu_0}{4\pi\|\boldsymbol{p}_i\|^5}\left(3\boldsymbol{p}_i\boldsymbol{p}_i^T - I\|\boldsymbol{p}_i\|^2\right)\boldsymbol{M} \qquad (2)$$

where $\boldsymbol{s}_i$ is the sensor's measurement axis in the capsule frame, which is known. The nonlinear least-squares Levenberg-Marquardt algorithm in MATLAB was implemented to estimate the capsule's pose by comparing the sensor data to the estimated field at each of the sensor positions using Eq. 2.

The spherical-actuator-magnet manipulator (Fig. 1) uses three omniwheels to provide a singularity-free rotating dipole field [12]. It is mounted on the end of a 6-DOF robot. A prototype capsule, 50.5 mm in length and 25 mm in diameter, was placed in a lubricated acrylic tube in which it is free to move, at a known position and orientation with accuracy of 2 mm and 10°, respectively, based on visual inspection.

The actuator magnet was rotated at 2 Hz around the **x**, **y**, and **z** axes, which resulted in step-out, with the actuator magnet's position held stationary. Data was collected at 100 Hz and wirelessly transmitted, in batches, at 20 Hz to a computer. Two rotations about each axis were combined, for a total of 3 s of data (1800 sensor measurements) to localize at a given position. For positions to test, we chose two orthogonal planes as depicted in Fig. 2.

RESULTS

The localization results are shown in Fig. 2. The total position error in mm and the orientation error in degrees are shown next to their corresponding position. The orientation error is in terms of the angle-axis representation. The average error across all points was 6.9 mm and 10.7°, the average computation time for the least-squares algorithm was 3.4 seconds. As expected, the position error tends to increase as the magnet is moved farther away from the capsule, due to reduced signal-to-noise. For both planes, the radial positions (along the **r** axis) result in more accurate position estimates than the axial positions (along the -**x** axis). We do not observe any clear trends in orientation error, but this could be partially due to our ground-truth orientation error having comparable values. Note that the two axial positions are the same in planes *A* and *B*, so the differences in the localization estimates give an indication of the variance that can be expected. This method assumes that the capsule has no net motion; some of the error is due to our experiments not respecting this assumption, as would be true in practice.

DISCUSSION

The accuracy obtained is likely to be sufficient for use with our previously published magnetic-actuation method [13]. It performs comparable to other 6-D localization methods; [7] has an average error of 5 mm in a slightly smaller 15 cm sphere. This localization method is not capable of localizing a synchronously rotating capsule because of the assumption that the capsule has no net motion. However, a simple control scheme involves pausing actuation at periodic intervals, and either increasing the rotation speed of the dipole field or rotating it around an orthogonal axis, either of which will cause the capsule to stop rotating synchronously, and after collecting a few rotations of data, continue propelling the capsule in a desired manner. No additional movement of the external dipole source is necessary. For the reported experiments, we arbitrarily chose to use two rotations about three orthogonal axes. Further investigation needs to be done to determine the relationship between the amount of data collected and the resulting accuracy. Subsequent to the reported experiments, we built a smaller version of the prototype capsule that is 36 mm in length and 13.5 mm in diameter. Although it is conceivable that the hardware size could be further reduced, we believe this will be sufficient for clinically realistic trials in future work.

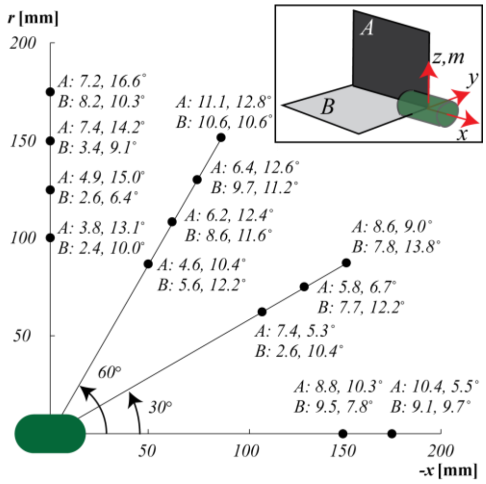

Fig. 2 The inset shows the two orthogonal planes tested. The capsule's **z** axis is aligned with its magnet's dipole axis **m**. On each plane, dots show positions tested. The position (mm) and orientation errors are shown next to the corresponding dot. The radial distance **r** refers to the **z** axis in plane *A* and the –**y** axis is plane *B.*

REFERENCES

[1] P. R. Slawinski, et al. Emerging issues and future developments in capsule endoscopy. *Tech Gastro Endo*, doi: 10.1016/j.tgie.2015.02.006, 2015.

[2] T.D. Than, et al. A review of localization systems for robotic endoscopic capsules. *IEEE Trans. Bio. Eng.*, 59(9):2387–2399, 2012.

[3] A.W. Mahoney and J.J. Abbott. Generating rotating magnetic fields with a single permanent magnet for propulsion of untethered magnetic devices in a lumen. *IEEE Trans. Robotics*, 30(2):411-420, 2014

[4] S. Song, et al. 6-D magnetic localization and orientation method for an annular magnet based on a closed-form analytical model. *IEEE Trans. Mag.*, 50(9):5000411, 2014.

[5] D. M. Pham and S.M. Aziz. A real-time localization system for an endoscopic capsule. In *IEEE Int. Conf. ISSNIP*, 1-6, 2014.

[6] M. Salerno, et al. Magnetic and inertial sensor fusion for the localization of endoluminal diagnostic devices. *I J CARS.*, (S1):229-235, 2012.

[7] C. Di Natali, et al. Real-time pose detection for magnetic medical devices. *IEEE Trans. Mag.*, 49(7):3524-3527, 2013.

[8] M. Salerno, et al. A discrete-time localization method for capsule endoscopy based on on-board magnetic sensing. *Meas. Sci, Technol.*, 23(1):015701, 2012.

[9] S. Yim and M. Sitti. 3-D localization method for a magnetically actuated soft capsule endoscope and its applications. *IEEE Trans. Robotics*, 29(5):1139-1151, 2013.

[10] M. Kim, et al. Position and orientation detection of capsule endoscopes in spiral motion. *Int. J. Prec. Eng. & Manu.*, 11(1):31-37, 2010.

[11] K. M. Popek, et al. Localization method for a magnetic capsule endoscope propelled by a rotating dipole field. *IEEE Int. Conf. Robotics & Auto.*, 5328-5333, 2013.

[12] S. E. Wright, et al. A spherical-magnet end-effector for robotic magnetic manipulation. *IEEE Int. Conf. Robotics & Auto.*, 2015, to appear.

[13] A. W. Mahoney and J. J. Abbott. Control of untethered magnetically actuated tools with localization uncertainty using a rotating permanent magnet. *IEEE Int. Conf. Biomedical Robotics & Biomech.*, 1632-1637, 2012.